Properties of Cyclic Nucleotide–gated Channels Mediating Olfactory Transduction

Activation, Selectivity, and Blockage

STEPHAN FRINGS, JOSEPH W. LYNCH, and BERND LINDEMANN

From the Department of Physiology, Universität des Saarlandes, D-6650 Homburg/Saar, Germany

ABSTRACT Cyclic nucleotide–gated channels (cng channels) in the sensory membrane of olfactory receptor cells, activated after the odorant-induced increase of cytosolic cAMP concentration, conduct the receptor current that elicits electrical excitation of the receptor neurons. We investigated properties of cng channels from frog and rat using inside-out and outside-out membrane patches excised from isolated olfactory receptor cells. Channels were activated by cAMP and cGMP with activation constants of 2.5–4.0 μM for cAMP and 1.0–1.8 for cGMP. Hill coefficients of dose–response curves were 1.4–1.8, indicating cooperativity of ligand binding. Selectivity for monovalent alkali cations and the Na/Li mole-fraction behavior identified the channel as a nonselective cation channel, having a cation-binding site of high field strength in the pore. Cytosolic pH effects suggest the presence of an additional titratable group which, when protonated, inhibits the cAMP-induced current with an apparent pK of 5.0–5.2. The pH effects were not voltage dependent. Several blockers of Ca^{2+} channels also blocked olfactory cng channels. Amiloride, D 600, and diltiazem inhibited the cAMP-induced current from the cytosolic side. Inhibition constants were voltage dependent with values of, respectively, 0.1, 0.3, and 1 mM at −60 mV, and 0.03, 0.02, and 0.2 mM at +60 mV. Our results suggest functional similarity between frog and rat cng channels, as well as marked differences to cng channels from photoreceptors and other tissues.

INTRODUCTION

Olfactory transduction in vertebrates is at least in part mediated by cyclic nucleotide–gated channels (cng channels) present in the sensory membrane of olfactory receptor cells (ORCs) (Trotier and MacLeod, 1986; Nakamura and Gold, 1987; Firestein and Werblin, 1989; Suzuki, 1989; Bruch and Teeter, 1990; Kolesnikov, Zhainazarov, and Kosolapov, 1990; Kurahashi, 1990; Firestein, Zufall, and Shepherd, 1991; Frings,

Address reprint requests to Dr. B. Lindemann, Department of Physiology, Universität des Saarlandes, D-6650 Homburg/Saar, Germany.

J. GEN. PHYSIOL. © The Rockefeller University Press · 0022-1295/92/07/0045/23 $2.00
Volume 100 July 1992 45–67

Benz, and Lindemann, 1991; Frings and Lindemann, 1991*a;* Lowe and Gold, 1991; Zufall, Firestein, and Shepherd, 1991; Zufall, Shepherd, and Firestein, 1991). These channels are directly activated by cAMP, released as a second messenger of the olfactory signal transduction pathway (Pace, Hanski, Salomon, and Lancet, 1985; Sklar, Anholt, and Snyder, 1986; Lowe, Nakamura, and Gold, 1989; Breer, Boekhoff, and Tareilus, 1990). Here we report that membrane patches excised from the ciliary knob of isolated frog and rat ORCs, i.e., from the membrane area at which sensory cilia arise, contain a high density of cng channels. Recording cyclic nucleotide–activated currents from this membrane allowed a more detailed investigation of olfactory cng channel properties and a comparison with cng channels from other tissues. Since the primary structure of the channel is known and functional expression of the channel protein has been achieved (Dhallan, Yau, Schrader, and Reed, 1990; Ludwig, Margalit, Eismann, Lancet, and Kaupp, 1990; Goulding, Ngai, Kramer, Colicos, Axel, Siegelbaum, and Chess, 1992), point mutations can now be performed with the channel protein (Altenhofen, Ludwig, Eismann, Kraus, Bönigk, and Kaupp, 1991). It is, therefore, necessary to establish the biophysical properties of the native channel in preparation for a structure–function analysis. In this study we analyzed the activation of cng channels from frog and rat ORCs by cyclic nucleotides, the selectivity and permeation by monovalent cations, and the blockage by pH and several Ca channel blockers. In subsequent papers (Frings, S., and B. Lindemann, manuscript in preparation; Lynch, J. W., and B. Lindemann, manuscript in preparation), blockage by divalent cations and their permeation through olfactory cng channels will be described.

Part of our results appeared in abstract form (Frings and Lindemann, 1991*b*).

METHODS

Cell Isolation (Frog)

Frogs (*Rana esculenta/ridibunda*) from Turkey were kept at 4°C in tap water during winter, or in a terrarium at 20–30°C during summer, where they were fed with crickets. Frogs were killed by decapitation, the skin covering the nose was removed, and the two dorsal olfactory mucosae were excised by cutting out the triangular plate of bone that supports the epithelium on each side of the septum. The epithelium was cut from the bone plates and washed in Ringer's solution (Table I). The two ventral mucosae were carefully lifted from the bone with bent forceps and also washed in Ringer's solution. The tissue was cut into pieces of ~1 mm^2 and transferred to papain solution (Ringer's solution containing 1 mg/ml papain, preactivated for 1 h with 5 mM *l*-cysteine) in which they were kept for 45 min at 35°C. After this, tissue pieces were washed several times in Ringer's solution to remove papain and then placed in sodium- and divalent cation-free dissociation solution (Table I) for 45 min at room temperature. Subsequent gentle trituration with a fire-polished Pasteur pipette released large numbers of single cells. Olfactory receptor cells were identified by their characteristic morphology: soma with remnant of the torn axon, dendrite with ciliary knob and up to 20 olfactory cilia (50–150 μm long). Cells were maintained in dissociation solution during the course of experiments (3–5 h). The papain treatment caused opening of the tight junctions and allowed ciliary knobs to swell. Gigaseals were easily formed on swollen knobs, and even outside-out patches could be obtained. Swelling of knobs was regularly observed when we used a papain batch purchased from Sigma Chemical Co. (St. Louis, MO) in 1988. (With subsequent batches, opening of tight junctions did not occur and could not be achieved by addition of trypsin, pronase E, pronase P,

collagenase, or use of insoluble papain. These cells had a narrow constriction just underneath their very small and highly refractile ciliary knobs, probably due to residual structures of the tight junction complex. Gigaseal formation was very difficult with such cells and the success rate was much lower.)

Cell Isolation (Rat)

Olfactory epithelium was obtained from septum and turbinates of adult rats. The isolation technique for rat olfactory receptor cells is described in detail in Lynch and Barry (1991). Briefly, tissue pieces were washed in Tyrode's solution (Table I) and then incubated in dissociation solution (Table I), containing 0.2 mg/ml trypsin, for 35 min at 37°C. After trituration with a wide-bored pipette (1.5 mm i.d.), isolated cells were transferred to the recording chamber and washed by superfusion with Tyrode's solution (Table I). Olfactory receptor cells showed distinct features including soma, dendrite, ciliary knob, and often several olfactory cilia of ~10 μm length.

TABLE I

Composition of Solutions (mM)

	Ringer	Tyrode	Dissociation		Patch		Pipette	
	Frog	Rat	Frog	Rat	Frog	Rat	Frog	Rat
NaCl	120	140	—	145	120	145	120	125
NaOH	4	4	—	8	25	5	25	25
KCl	3	5	3	5	—	—	—	—
$CaCl_2$	1	2	—	—	—	—	—	—
$MgCl_2$	2	1	—	—	—	—	—	—
HEPES	10	10	10	10	10	10	10	10
Glucose	5	10	5	10	—	—	—	—
Pyruvate	5	—	5	—	—	—	—	—
EGTA	—	—	—	—	10	—	10	10
EDTA	—	—	2	—	—	—	—	—
NMDG-Cl	—	—	120	—	—	—	—	—
pH	7.4	7.4	7.4	7.4	7.4	7.4	7.4	7.4

Recording Chamber

A Sylgard chamber was glued onto a standard microscope slide and divided into two separate compartments connected by a narrow channel. One compartment, which was constantly perfused with dissociation solution, served for storage of cells during experiments and for obtaining on-cell patches. The other compartment was equipped with a number of perfusion inlets allowing exposure of excised patches to different test solutions. After formation and excision of patches, pipettes were transferred through the channel to the second compartment and positioned in front of one of the perfusion tubes. Solutions were changed rapidly (< 100 ms) by moving the perfusion tubes with the microscope stage.

Patch-Clamp Recording from Ciliary Knob Membrane

Fire-polished patch pipettes with resistances of 15–25 MΩ were used to obtain gigaseals on the ciliary knobs of the olfactory receptor cells of both species. Standard patch-clamp techniques were used (Hamill, Marty, Neher, Sakmann, and Sigworth, 1981) and patches were excised by

brief air exposure. Pipettes were filled with patch solution (Table I) if not stated otherwise. Potassium was omitted to avoid contamination by K channels present in the knob membrane. Currents were measured under voltage-clamp conditions by applying 4–16 voltage ramps to the membrane patch. Voltages and digitally averaged currents were stored in an IBM-AT computer and monitored on-line. Membrane patches from frog ORCs could usually be investigated in a voltage range of ±100 mV, while recording from rat ORCs was limited to ±60 mV because of unstability of patches at higher voltages. Current–voltage (*I-V*) curves of cng channels in inside-out patches were obtained by subtracting the leak currents recorded in the absence of cyclic nucleotides. In outside-out recordings, cAMP was included in the pipette solution and leak current was estimated by using one or both of the following procedures: (*1*) Inward currents were recorded at large negative membrane voltages (−80 to −100 mV) in the presence of the impermeable cation *N*-methyl-D-glucamine ($NMDG^+$) in the bath solution. In these experiments, patch conductance with mucosal $NMDG^+$ was usually < 5% of conductance in the presence of Na^+. (*2*) To obtain complete control *I-V* curves in outside-out patches, cAMP-induced current was blocked by reducing bath pH to 3.0 for several minutes (this results in a complete block of cng channels; see below), after which the *I-V* curve of the residual current was used as control. For activation of cng current, unless otherwise specified, a saturating concentration of 20–40 μM (rat) of 100 μM (frog) cAMP was used. Membrane potentials are given for the internal with respect to the external membrane surface.

Materials

Papain (cystallized twice, 10–20 U/mg), adenosine 3′:5′-cyclic monophosphate (cAMP, sodium salt), 8-(4-chlorophenylthio)-adenosine 3′:5′-cyclic monophosphate (cpt-cAMP), guanosine 3′:5′-cyclic monophosphate (cGMP, sodium salt), L-cysteine, and *N*-methyl-D-glucamine (NMDG) were obtained from Sigma Chemical GmbH (Deisenhofen, Germany), amiloride from Sharp Dohme GmbH (Munich, Germany), D 600 from Knoll AG (Ludwigshafen, Germany), *d-cis*-diltiazem and *l-cis*-diltiazem from Goedecke AG (Berlin, Germany), and trypsin from GIBCO (Eggenstein, Germany).

RESULTS

Activation by Cyclic Nucleotides

Membrane patches excised from areas of either soma, dendrite, or ciliary knob of olfactory receptor cells (Fig. 1 *A*) had very different densities of cng channels. Patches from soma and dendritic membrane had no or very few channels and could therefore be used for investigation of single channel parameters. With low concentrations of divalent cations on both sides of the membrane (Table I, patch solution), single channel conductances were 12–15 pS in both frog and rat. The channels could be activated by cAMP and cGMP (Fig. 1 *C*) and were blocked by amiloride applied to the cytosolic side of the patches (Fig. 1 *D*). Patches from ciliary knobs, in contrast, showed a much higher density of cng channels. Cyclic nucleotide–activated membrane conductances in knob patches were usually in the range of 5 nS in frog and 2 nS in rat, but were occasionally as large as 25 nS in frog and 10 nS in rat, indicating the activity of > 1,000 cng channels per patch (Fig. 1 *B*). Because most effects of modulators of the cyclic nucleotide–activated current could be more accurately measured using large current signals, we concentrated on studying excised patches of knob membrane. Application of cAMP or cGMP to the cytosolic side of membrane patches resulted in a graded increase of patch current which saturated at concentra-

tions of 10–30 μM. *I-V* relationships of cyclic nucleotide–induced currents of both species showed weak outward rectification (Fig. 2, *A–D*). The rectification ratio ($RR = I_{+V}/I_{-V}$) was strongly dependent on cyclic nucleotide concentration in the range of 1–10 μM, and was also influenced by the membrane voltage (inset in Fig. 2 *A*). The rectification ratio of 7.5 on the 100-mV curve means that, at the given

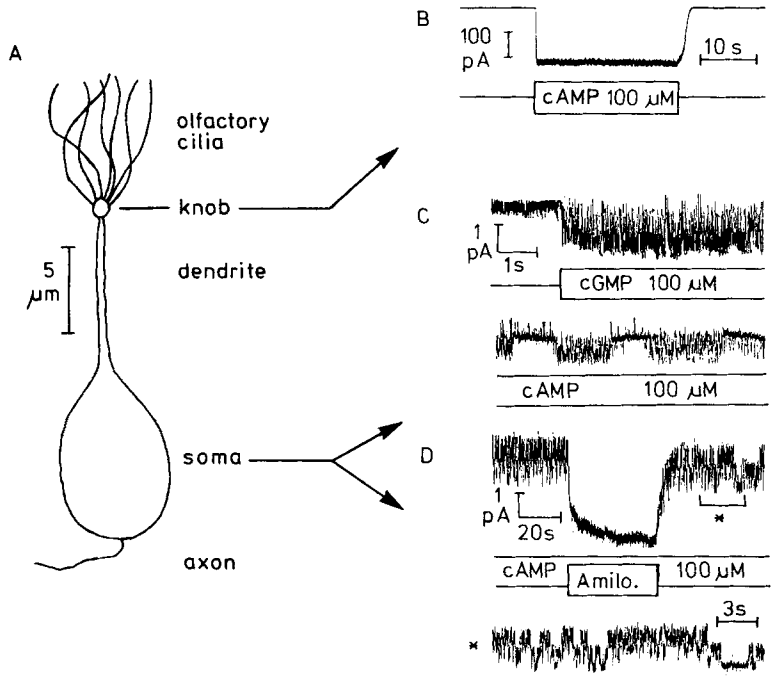

FIGURE 1. (*A*) Schematic representation of an olfactory receptor neuron isolated from the olfactory epithelium. Olfactory cilia in isolated frog ORCs usually have cilia of 50 μm length which often are motile. Cilia from isolated rat ORCs appear much thinner, are ~10 μm long, and are not motile. (*B*) Inward current induced by 100 μM cAMP applied to the cytosolic side of a frog knob membrane inside-out patch. Frog patch solution was used in the bath, and the membrane voltage was −30 mV. (*C*) Activation of two cng channels in an inside-out patch from frog soma membrane by 100 μM cGMP (*upper trace*) and 100 μM cAMP (*lower trace*). The lower trace shows a section where single channel events are discernible. Symmetrical patch solution was used at a membrane voltage of −50 mV. Single channel current (0.7 pA) indicates a conductance of 14 pS. (*D*) Inside-out recording from a frog soma patch showing activity of 5 cng channels activated by 100 μM cAMP at +40 mV. Single channel current (0.6 pA) indicates a conductance of 15 pS. Application of 500 μM amiloride during the indicated time blocked the channels reversibly. Lower trace shows current fluctuations at a sixfold extended time scale.

cAMP concentration, the cAMP-induced current at +100 mV was 7.5 times larger than the current at −100 mV. Current activation by cyclic nucleotides was rapid and readily reversible (Fig. 1 *B*). The current showed no run-down; i.e., the maximally activated conductance did not change during the course of experiments (usually ~30 min). Dose–response relationships for cyclic nucleotides (Fig. 2, *E* and *F*) show that

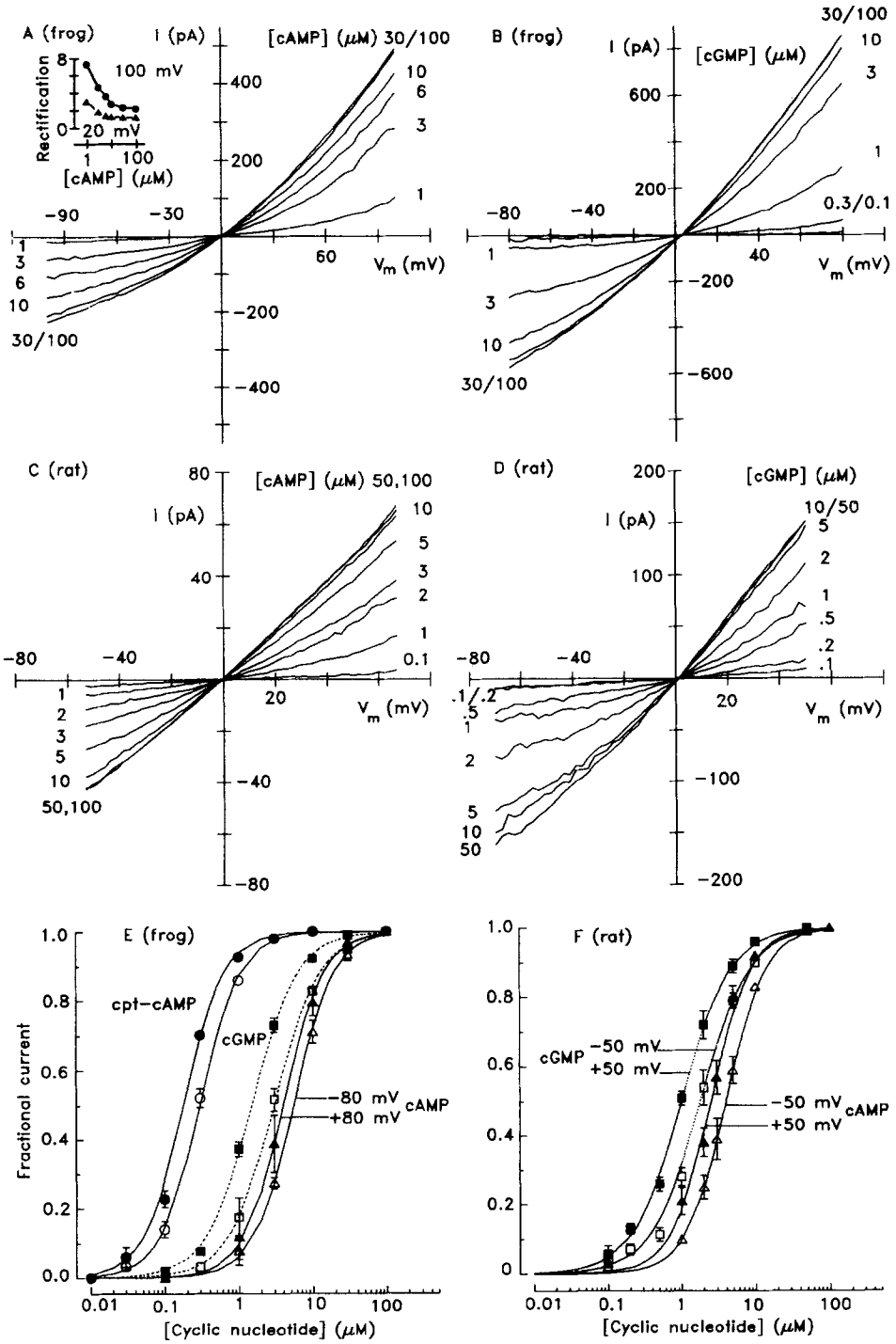
A (frog)
I (pA)
[cAMP] (μM) 30/100
Rectification
100 mV
20 mV
[cAMP] (μM)
B (frog)
[cGMP] (μM)
C (rat)
[cAMP] (μM) 50,100
D (rat)
[cGMP] (μM)
E (frog)
cpt-cAMP
cGMP
−80 mV cAMP
+80 mV
Fractional current
[Cyclic nucleotide] (μM)
F (rat)
cGMP −50 mV
+50 mV
−50 mV cAMP
+50 mV
[Cyclic nucleotide] (μM)

FIGURE 2

TABLE II

Activation of Olfactory cng Channels

	cAMP			cGMP			cpt-cAMP		
	K_M	HC	n	K_M	HC	n	K_M	HC	n
Frog (+80 mV)	4.0	1.6	3	1.5	1.4	3	0.17	1.6	2
Frog (−80 mV)	5.5	1.6	3	3.0	1.4	3	0.3	1.6	2
Rat (+50 mV)	2.5	1.8	8	1.0	1.3	5	—	—	—
Rat (−50 mV)	4.0	1.8	8	1.8	1.3	5	—	—	—

K_M, concentration for half-maximal activation; HC, Hill coefficient; n, number of observations.

cGMP was somewhat more potent than cAMP and the activation constants of both nucleotides were slightly voltage dependent, being somewhat lower at positive membrane voltages. Concentrations for half-maximal activation (K_m) as well as the Hill coefficients used to fit the dose–response curves (HC) are given in Table II. In frog, the cAMP analogue chlorophenylthio-cAMP (cpt-cAMP) was ~20 times more effective than cAMP in activating cng channels.

Selectivity for Monovalent Cations

The ability to discriminate between alkali monovalent cations was examined for the cng channels of both species. In the case of the rat, this was performed in inside-out patches where the pipette contained rat pipette solution (Table I), corresponding to an extracellular Na^+ concentration of 150 mM. The intracellular membrane surface was exposed successively to solutions containing similar concentrations of either Na^+, K^+, Li^+, Rb^+, or Cs^+ ions. Voltage ramps were applied in both the presence and absence of a saturating concentration (40 μM) of cAMP and the difference revealed the *I-V* relationship under each biionic condition. Liquid junction potential corrections were calculated as described previously (Barry and Lynch, 1991) and applied as follows: Na^+, 0 mV; K^+, +4.3 mV; Li^+, −2.5 mV; Cs^+, +3.7 mV; Rb^+, +3.6 mV. Examples of currents recorded from one patch are shown in Fig. 3 *A*. Measurement of the reversal potential in each cation solution gives a measure of the permeation sequence relative to Na^+. The results for each cation were averaged from 5–10

Figure 2. (*opposite*) (*A, B*) *I-V* curves of cyclic nucleotide–activated currents from frog knob membrane inside-out patches recorded with symmetrical frog patch solution. Various concentrations of cAMP (*A*) and cGMP (*B*) were applied to the cytosolic side of the membrane. Inset in *A* shows rectification ratio (see text) as a function of cAMP concentration at 100 mV (*circles*) and 20 mV (*triangles*). (*C, D*) *I-V* curves from rat knob membrane patches with different concentrations of cAMP (*C*) and cGMP (*D*) applied to the cytosolic side of patches in symmetrical rat patch solution. (*E, F*) Dose–response relationships of activation by cyclic nucleotides of cng channels in frog (*E*) and rat (*F*) knob membrane patches. Dashed curves are for cGMP, and solid curves are for cAMP and chlorophenylthio- (cpt-) cAMP. All nucleotides tested were slightly more effective at positive membrane voltages (*filled symbols*). Parameters used for fitting the curves are given in Table I. Data were derived from *I-V* curves as shown in *A–D*. Patch solution was used on both sides of the membrane.

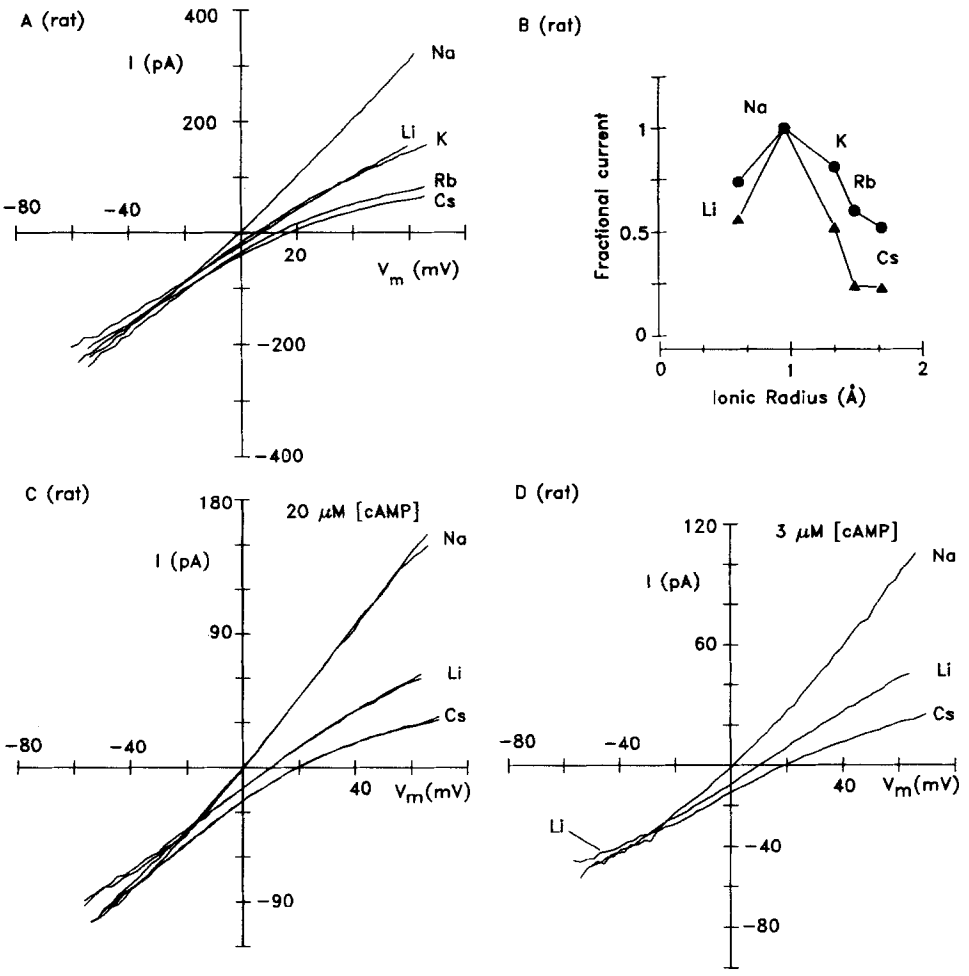

FIGURE 3. Ionic selectivity of rat cng channels. (*A*) *I-V* curves from an inside-out patch from rat ciliary knob membrane. Current activated by 40 μM cAMP was recorded with 150 mM Na in the pipette (rat pipette solution) and the same concentration of test ions in the bath (with 10 mM HEPES, and Tris added to obtain pH 7.4). Reversal potentials were used to calculate permeability ratios, while the conductance sequence was derived from currents at +50 mV. (*B*) Plot of permeability (*circles*) and conductance (*triangles*) sequences against the ionic radius of each tested ion. Each data point represents the average value from 5–10 patches. (*C, D*) Ionic selectivity at two cAMP concentrations. Reducing cAMP from 20 μM (*C*) to 3 μM (*D*) did not significantly alter permeability or conductance ratios. *C* shows *I-V* curves before and after exposure to 3 μM cAMP. Note the slight inhibition of Na^+ current at negative membrane potentials by cytosolic Li^+.

patches and gave the following sequence of permeation ratios relative to Na^+:

$$Na^+ (1):K^+ (0.81):Li^+ (0.74):Rb^+ (0.60):Cs^+ (0.52).$$

The conductance sequence for outward currents measured relative to Na^+ at +50 mV was as follows:

$$Na^+ (1):Li^+ (0.56):K^+ (0.52):Rb^+ (0.24):Cs^+ (0.23),$$

which is similar to the permeation sequence except that the positions of Li^+ and K^+ are reversed. However, since the conductance curves for K^+ and Li^+ generally crossed each other near +40 mV (Fig. 3 *A*), at less positive voltages the sequences were the same. This series corresponds to the Eisenman sequence *X* (Eisenman and Horn, 1983) for a relatively high field strength site. A plot of the relative permeabilities and conductances versus the cation radius is shown in Fig. 3 *B*.

Alkali cation permeation studies of the cGMP-gated channel in photoreceptors have shown that Li^+ is somewhat anomalous in its permeation properties. That is, although equilibrium selectivity for Li^+ is large, the conductance is small. This suggests binding of Li^+ to a binding site in the channel (Furman and Tanaka, 1990; Menini, 1990; Lühring, Hanke, Simmoteit, and Kaupp, 1990). This effect is not strong in the rat cng channel. However, Na^+ currents at negative membrane potentials in the presence of internal Li^+ were consistently less than in the presence of other internal cations (Fig. 3 *C*). This suggests that Li^+ does interfere with the passage of other cations through this channel, but to a lesser degree than in the photoreceptor channel.

Several authors have suggested that the binding of an increased number of cyclic nucleotide molecules to the receptor site opens the channels to a progressively larger conducting state, facilitating the permeation of both monovalent (Ildefonse and Bennett, 1991) and divalent (Colamartino, Menini, and Torre, 1991) cations. If this is the case, the monovalent cation permeation sequence may also vary with cAMP concentration. To test this hypothesis, the permeabilities of both Cs^+ and Li^+ relative to Na^+ were compared at 3 and 20 μM cAMP. Cs^+ and Li^+ were chosen, as they are, respectively, the largest and smallest ions in the tested series, and comparison of the changes in their relative permeation properties may be expected to be a sensitive assay of changes in the selectivity filter of the channel. Experiments were performed as described above and results of a typical experiment are shown in Fig. 3, *C* and *D*. Fig. 3 *C* displays *I-V* relationships in 20 μM cAMP both before and after measurement in 3 μM cAMP (shown in Fig. 3 *D*). Although *I-V* relationships in 3 μM cAMP display the expected increase in outward rectification (cf. Fig. 2), there was essentially no difference in either the reversal potential or relative magnitudes of macroscopic outward currents. These results were confirmed in each of three other patches.

In the frog, relative conductance sequences were studied using pipette solution with Na^+ replaced by the impermeable cation $NMDG^+$ (100 mM). The bath contained 100 mM of one of the tested monovalent cations, together with 100 μM cAMP. Examples of outward currents recorded from one patch are displayed in Fig. 4 *A*. The outward rectification is caused by the inability of $NMDG^+$ to permeate the

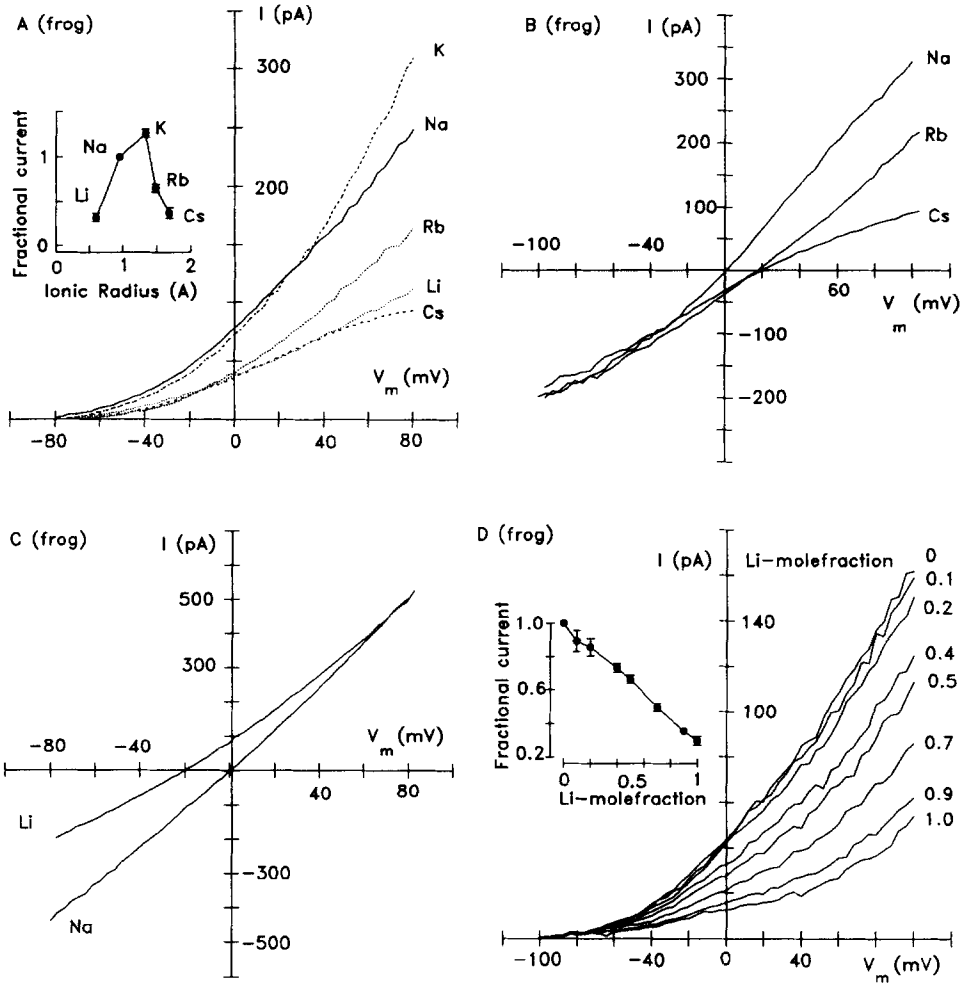

FIGURE 4. Ionic selectivity of frog cng channels. (*A*) Currents carried by various alkali cations through frog cng channels activated by 100 μM cAMP. An inside-out patch from knob membrane was used with 100 mM NMDG-Cl in the pipette (with 10 mM HEPES and 1 mM EGTA, pH 7.4). The inability of $NMDG^+$ to cross the channels causes outward rectification of *I-V* curves. Alkali cations were applied to the cytosolic side at 100 mM (these solutions, as well as those in *B*, *C*, and *D*, also contained: 10 mM HEPES, 1 mM EGTA, and 7 mM Tris, pH 7.2. All cations were added as chloride salts). The inset shows a plot of the fractional current of each ion tested, relative to Na^+ current, against ionic radius (mean of three patches). (*B*) Reversal potential measurements with Rb^+ and Cs^+ in an inside-out patch with 100 mM Na^+ in the pipette and 100 mM of the indicated cation in the bath. Liquid junction potentials are compensated. (*C*) Reversal potential measurement with Li^+ in an outside-out patch from the knob. The pipette contained 100 mM Na^+ and 100 μM cAMP, with 100 mM Na^+ or Li^+ in the bath solution. The control *I-V* curve was obtained by blocking cng channels at pH 3 (see Methods) and subtracted. (*D*) Mole-fraction experiment with an inside-out patch with 100 mM Na^+ in the pipette. The composition on the cytosolic side of the patch was changed according to the Li^+ mole-fraction values indicated. Li^+ mole-fraction = $[Li^+]/([Li^+] + [Na^+])$. The inset shows the monotonic decline of cAMP-induced current as the Li^+ mole-fraction increases (mean of two patches).

channels. The conductance sequence at +80 mV was (mean of three patches):

$$K^+ (1.26):Na^+ (1):Rb^+ (0.65):Cs^+ (0.37):Li^+ (0.32).$$

At less positive membrane potentials, the difference between the Na^+ and K^+ conductances, as well as between the Cs^+ and Li^+ conductances, decreased even more. This series corresponds to the Eisenman sequence VI, typical for a binding site with moderately high field strength. Permeability ratios of Rb^+ and Cs^+ were measured in two inside-out patches with 100 mM Na^+ in the pipette and the same concentration of either Rb^+ or Cs^+ in the bath (Fig. 4 *B*). After correcting for liquid junction potentials, reversal potentials were +17 and +8 mV with Rb^+, and +20 and +15 mV with Cs^+, corresponding to permeability ratios of $P_{Rb}/P_{Na} = 0.51$ and 0.73, and $P_{Cs}/P_{Na} = 0.46$ and 0.56. Lithium permeability was measured in an outside-out patch with 100 mM Na^+ in the pipette (Fig. 4 *C*). Exchanging mucosal (bath) Na^+ for Li^+ shifted the reversal potential to −20.5 mV, indicating a permeability ratio of $P_{Li}/P_{Na} = 0.49$. Thus, permeability ratios for Li^+ and Cs^+ were significantly lower than conductance ratios, while, in the case of Rb^+, permeability and conductance ratios were similar. A plot of the conductance ratios against the ionic radius of the transported ions is shown as an inset in Fig. 4 *A*.

One method of detecting the presence of several binding sites in a pore, through which ions have to move in single file, is to measure the mole-fraction behavior of ion currents (Almers and McCleskey, 1984; Hess and Tsien, 1984). Single-file diffusion is suggested when the measured current passes through a distinct minimum, as one ion is progressively replaced by another (anomalous mole-fraction behavior), while a monotonic function is observed if a single binding site is involved. Since the high permeability and low conductance of Li^+ in frog cng channels suggest binding to a site with relatively high affinity, Li^+ was a likely candidate to reveal single-file diffusion in a mole-fraction experiment. In frog cng channels, the fractional current carried by various mixtures of Na^+ and Li^+ declined monotonically with increasing Li^+ mole-fraction ($[Li^+]/([Li^+] + [Na^+])$; Fig. 4 *D*). Thus, the Li/Na mole-fraction behavior did not indicate more than one binding site within the channel pore.

Inhibition by Cytosolic Acidification

When the pH of the solution bathing the cytosolic side of inside-out patches was reduced below 7.0, cAMP-induced current was inhibited rapidly and reversibly (Fig. 5, *A* and *B*). Current inhibition was not voltage dependent, being almost complete at pH 4.0. The apparent pK was 5.2 (SD = 0.24, $n = 5$) in frog and 5.1 (SD = 0.07, $n = 2$) in rat. While pH effects on the cytosolic side of the channels were rapid, pH steps applied to the mucosal surface of outside-out patches caused much slower current inhibition, taking 5–6 min to develop fully (Fig. 5 *C*). Apparently, the titratable site was located on the cytosolic side of the membrane and mucosal H^+ ions had to cross the membrane, possibly through cng channels, before binding to this group. The nucleotide binding site on the cytosolic surface of the channel protein (Kaupp, 1991) might be affected by the binding of protons. To test for the possibility that protons interact competitively with cAMP binding to the channel, pH was first reduced to 5.0 in the presence of 100 μM cAMP. At the same pH, cAMP

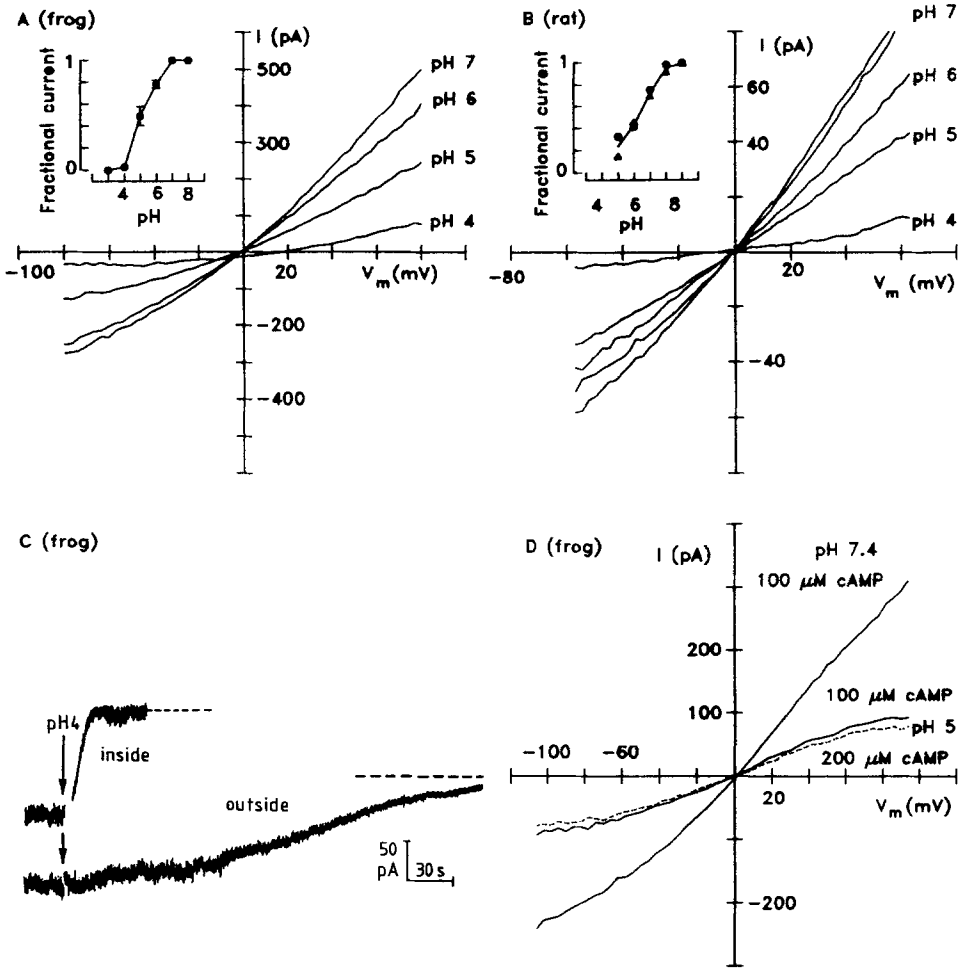

FIGURE 5. (*A*) Cytosolic acidification inhibits cAMP-induced current in a frog knob inside-out patch. Test solutions contained (mM): 120 NaCl, 20 NaOH, 10 Na_2HPO_4, 2 NaH_2PO_4, 10 EGTA, and 0.1 cAMP, plus different amounts of 0.5 mM HCl, containing 120 mM NaCl, to obtain pH values between 3.0 and 8.0. The pipette solution had a pH of 7.0. (*Inset*) Titration curve for frog cng current showing an apparent pK of 5.2 (currents measured at +80 mV; mean of five patches). (*B*) Effect of cytosolic acidification on cAMP-induced current in rat knob membrane. Solutions as in *A*. (*Inset*) Titration curve of rat cng channels measured in two patches at +60 mV. The apparent pK is 5.0. (*C*) Difference of time course of current inhibition induced by acidification at the inside or outside of frog knob membrane. Dashed lines represent zero cAMP-induced current. On changing bath solution from pH 7.0 to 4.0 (time for solution change was < 100 ms), cAMP-induced current was completely blocked within 18 s in the inside-out patch, while blockage in the outside-out patch took 320 s to become complete. (*D*) *I-V* curves of cAMP-induced current at pH 7.4 and 5.0, showing current inhibition by 60% through acidification. Increasing cAMP from 100 to 200 μM at pH 5.0 did not attenuate current inhibition.

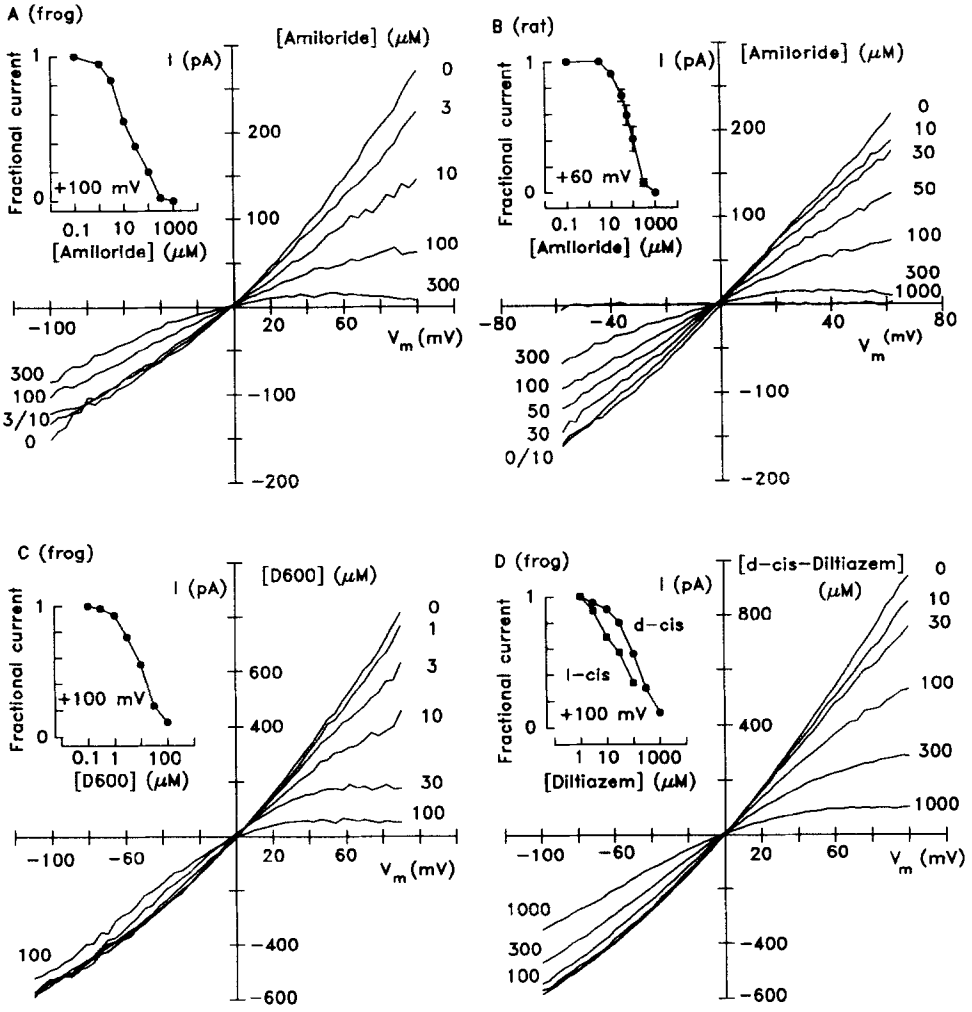

FIGURE 6. Inhibition of cAMP-induced current by Ca channel blockers. (*A*, *B*) Amiloride applied to the cytosolic side of frog (*A*) and rat (*B*) knob membrane patches. Current rectification in the presence of the drug indicates voltage-dependent blockage of cng channels. Insets show dose–response curves for amiloride block with inhibition constants (K_i) of 17 μM (at +100 mV) in frog and 70 μM (at +60 mV) in rat. Symmetrical patch solutions were used with 100 μM cAMP in the bath. (*C*, *D*) Inhibition of cng channels by D 600 and diltiazem. *I-V* curves were recorded from frog knob membrane inside-out patches in the presence of 100 μM cAMP in the bath. Both D 600 (*C*) and diltiazem (*D*) inhibited cAMP-induced current much better at positive membrane potentials. The insets show dose–response relationships of the drugs at +100 mV with inhibition constants (K_i) of 12 μM for D 600 and 70 and 120 μM for *l-cis*-diltiazem and *d-cis*-diltiazem, respectively.

concentration was then raised to 200 μM but no release of the current inhibition was observed (Fig. 5 *D*). Thus, there was no evidence for protons either competing with cAMP binding to cng channels, or reducing cAMP activity. Both effects should have been at least partially compensated by doubling the cAMP concentration.

Inhibition by Organic Blockers

When the cytosolic side of excised knob membrane patches was exposed to amiloride, the cAMP-induced current was inhibited rapidly and reversibly (Fig. 6, *A* and *B*). This inhibition was voltage dependent, being strongest at positive membrane potentials, when the positively charged amiloride was driven into the channel. The amiloride inhibition constant K_i decreased from 400 μM at −100 mV to 17 μM at +100 mV (Fig. 7). With a voltage displacement of 58 mV, K_i changed 2.6-fold in frog and 1.7-fold in rat, suggesting that the binding site in the cng channel was situated at

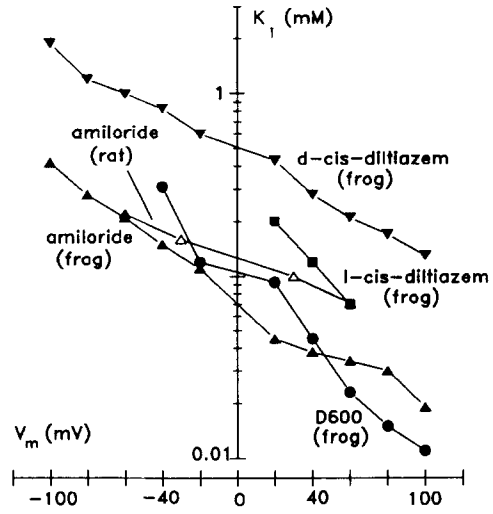

FIGURE 7. Voltage dependence of inhibition constants (K_i) for compounds inhibiting cng current. Inside-out patches were used with patch solution on both sides of the membrane. Current through cng channels was activated by 100 μM cAMP and several concentrations of blockers were added to the bath. Dose–response curves were generated for each membrane potential indicated, from which blocker concentrations for half-maximal inhibition (K_i) were obtained.

an apparent electrical distance of 0.41 (frog) and 0.23 (rat) from the inner membrane surface. Amiloride applied to the external side of outside-out membrane patches inhibited cAMP-induced current with a much slower time course and required higher concentrations (not shown), suggesting that the binding site was not directly accessible from the external membrane surface. The slow blocking effect seen may be due to amiloride penetrating the lipid phase of the membrane in the uncharged form, thus reaching the binding site through the unstirred layer on the inner side of the membrane.

In rat, cAMP-activated currents in 2 out of 11 knob patches were not sensitive to amiloride: application of 300 μM amiloride to the cytosolic side of these patches did not affect cng channels. To ascertain the validity of this observation, the same amiloride solutions were tested on other patches where they blocked cng currents in the typical fashion.

Two other Ca channel blockers tested also inhibited cng channels at relatively high concentrations. D 600 (methoxy-verapamil) and diltiazem inhibited cAMP-induced current in a voltage-dependent manner from the cytosolic side of the patch (Fig. 6, *C* and *D*). D 600 blocked with a K_i of 200 μM at −20 mV and 12 μM at +100 mV. *l-cis*-diltiazem was slightly more potent than *d-cis*-diltiazem: at +50 mV the K_i was 200 μM for the *d-cis* and 70 μM for the *l-cis* isomer. The voltage dependence of inhibition constants for the blockers tested is shown in Fig. 7.

DISCUSSION

Activation by Cyclic Nucleotides

Cng channels are concentrated in the sensory membrane of olfactory receptor cells. Since the partition between apical (sensory) and basolateral membrane, the tight junctions, is located on the proximal part of the ciliary knob (Reese, 1965; Menco, 1980), it may be assumed that the distal part of the knob forms a continuum with the sensory cilia, with essentially the same membrane proteins. Nakamura and Gold (1987) found cng channels in the ciliary membrane of toad olfactory receptor cells with a density similar to that which we found in patches from the apical knobs of both frog and rat. Kurahashi and Kaneko (1991) demonstrated by noise analysis a density of cng channels in toad ciliary membrane of 2,400/μm², while the density in the membrane of dendrite and soma was 6/μm². We found that the high channel densities in knob patches were useful for studying cyclic nucleotide–activated currents. Patches from the ciliary membrane were too difficult to obtain for extensive investigations, mainly due to the small diameter (0.1–0.2 μm) of the cilia.

The cng channels from frog and rat olfactory receptor cells share a number of properties with cyclic nucleotide–activated channels found in a variety of other cells. In particular, direct activation by cyclic nucleotides, voltage-dependent activation constants in the lower micromolar range, cooperativity of ligand binding indicated by Hill coefficients > 1, outward rectification of *I-V* curves, and lack of current inactivation characterize this family of ligand-controlled ion channels. For comparison, Table III summarizes several properties of olfactory cng channels from different species. Activation constants measured with frog cng channels were in accordance with results from previous work on frog (Kolesnikov et al., 1990), toad (Nakamura and Gold, 1987), and catfish (Bruch and Teeter, 1990), while cng channels from salamander ORCs have a somewhat lower affinity for cAMP (Zufall et al., 1991). Data from native mammalian olfactory cng channels have not been published so far. In our experiments, channel activation was very similar to amphibian olfactory cng channels. There is, however, a striking difference in the cAMP affinity between native and cloned cng channels from rat. Dhallan et al. (1990) found a 17 times higher activation constant for cAMP in the cloned rat channel, while cGMP affinity was similar to our observations. We have no explanation for this discrepancy, but it should be noted that cloned bovine olfactory cng channels also have a comparably low affinity for cAMP (64 μM), and cloned catfish cng channels are ~16 times less sensitive to cyclic nucleotides than the native channels from this animal (see Table III). It seems possible, therefore, that the channel protein undergoes posttranslational or cotranslational modification in the native cell but not in the expression

system, an interpretation that could account for differences between native and reconstituted cloned cng channels. Posttranslational modification could involve proteolysis, as suggested for cng channels from photoreceptors (Hurwitz and Holcombe, 1991; Molday, Molday, Dosé, Clark-Lewis, Illing, Cook, Eismann, and Kaupp, 1991), and it may also influence the affinity of the channel for cyclic nucleotides.

Alternatively, it is conceivable that cloned, reconstituted channels may lack a subunit that determines properties of the native channel, or that only a certain isotype of olfactory cng channel is functional in the expression systems. Nakamura

TABLE III

Properties of Olfactory cng Channels of Various Species

Cell type	Conductance* pS	K_M (cAMP)‡ (V_m, HC)	K_M (cGMP)‡ (V_m, HC)	P_K/P_{NA}	Reference
Catfish (native)	44	2–3	2–3	1	Bruch and Teeter, 1990
Catfish (cloned)	55	42 (−, 1.4)	40 (−, 1.3)	—	Goulding et al., 1992
Salamander (native)	45	20 (−50, 2.1)	4 (−50, 2.1)	1	Zufall et al., 1991
Toad (native)	—	3.4 (0, 1.5)	1.5 (0, 1.5)	1	Nakamura and Gold, 1987
Frog (native)	19	3.4	2.1	1	Kolesnikov et al., 1990
Frog (native)	12–15	4.0 (+80, 1.6)	1.5 (+80, 1.4)	1.1	This paper
Rat (native)	12–15	2.5 (+50, 1.8)	1.0 (+50, 1.3)	0.8	This paper
Rat (cloned)	—	68 (+40, 2.0)	2.4 (+40, 2.0)	0.8	Dhallan et al., 1990
Cattle (cloned)	—	64 (+80, 2.9)	1.5 (+80, 2.2)	—	Altenhofen et al., 1991

*Single channel conductance in the absence of divalent cations.

‡Concentration for half-maximal activation in micromolar with membrane potential (V_m) and Hill coefficient (HC) in brackets.

and Gold (1987) reported evidence for a subpopulation of cng channels with lower affinity for cAMP and cGMP in toad ORCs. These channels had activation constants similar to values found with cloned cng channels.

The slight voltage dependence of cyclic nucleotide dose–response curves was also reported for photoreceptor cng channels. Haynes, Kay, and Yau (1986), and Karpen, Zimmerman, Stryer, and Baylor (1988) observed that the cGMP binding constant was smaller at positive membrane potentials and suggested two distinct conformational states with different cGMP affinities. The state with the higher affinity would be favored at positive membrane voltages.

Channels conducting the dark current in vertebrate photoreceptors show a high degree of structural homology to the cng channel from olfactory epithelium (Ludwig et al., 1990). Photoreceptor channels are activated by cGMP with K_M values in the range of 10–80 μM, cAMP is much less effective (K_M is 1,849 μM in cloned bovine photoreceptor channels), single channel conductance is between 6 and 38 pS, and the channels do not discriminate between Na and K (Haynes et al., 1986; Zimmermann and Baylor, 1986; Cook, Zeilinger, Koch, and Kaupp, 1986; Matthews, 1987; Hanke, Cook, and Kaupp, 1988; Kaupp et al., 1989; Yau and Baylor, 1989; Haynes and Yau, 1990; Altenhofen et al., 1991; Ildefonse and Bennett, 1991; Quandt, Nicol, and Schnetkamp, 1991). Thus, there are significant differences in the properties of the cng channels involved in visual and olfactory transduction with regard to their activation by cyclic nucleotides. Furthermore, recently discovered cng channels in mammalian cochlear hair cells are activated by cAMP (and not by 1 mM cGMP; Kolesnikov, Rebrik, Zhaiazarov, Tavartkiladze, and Kalamkarov, 1991), while cng channels from chick pineal gland show the reverse selectivity for cyclic nucleotides (Dryer and Henderson, 1991). In summary, while conducting properties of cng channels are similar (see below), sensitivity to cyclic nucleotides seems to be specific for each tissue.

The cAMP analogue cpt-cAMP was ~20 times more potent in activating frog olfactory cng channels than cAMP itself. This higher affinity, together with the better membrane permeability, make this compound suited for extracellular application. Thus, 100 μM cpt-cAMP applied to the ciliary surface of the frog olfactory epithelium increased the rate of action potentials from 1.4 to 5 per second (Frings and Lindemann, 1991*a*), while applying 5 mM cAMP had no effect on spike rate. Interestingly, a similar difference in affinity between cAMP and its cpt analogue was reported for cAMP-dependent protein kinase in rat liver (Miller, Beck, Simon, and Meyer, 1975). Similar effects were shown for the cGMP analogue 8Br-cGMP in intact frog olfactory epithelium (Frings and Lindemann, 1991*a*) and by Zimmermann, Yamanaka, Eckstein, and Baylor (1985) in photoreceptor cells, where the derivatized nucleotide was also more potent. Experiments with cyclic nucleotide analogues may in the future assist in the understanding of ligand binding to cng channels.

Selectivity for Monovalent Cations

Our results from rat and frog ORCs indicate that their cng channels are nonselective cation channels, discriminating poorly between alkali cations, particularly between the physiologically relevant ions Na^+ and K^+. Lack of anomalous Li/Na mole-fraction behavior suggests a pore with a single binding site, and the conductance sequence indicates that this site has a relatively high field strength.

All investigations into the ionic selectivity of olfactory cng channels have so far shown permeability ratios P_K/P_{Na} in the range of 0.8–1.1 (Nakamura and Gold, 1987; Suzuki, 1988; Bruch and Teeter, 1990; Dhallan et al., 1990; Kolesnikov et al., 1990; Kurahashi, 1990). Li^+ was often reported to have a permeability similar to that of Na^+ and K^+, in agreement with our results from the rat. The current carried by Li^+ is, however, smaller than the Na^+ current, indicating that Li^+ binds to the channel with higher affinity, dwelling longer at the binding site where it competes with Na^+. Permeability sequences in photoreceptor cng channels were generally similar to the

sequences reported here (Hodgkin, McLaughton, and Nunn, 1985; Kaupp et al., 1989; Furman and Tanaka, 1990; Lühring et al., 1990; Menini, 1990). In particular, photoreceptor cng channels were found to contain a single, high field-strength site to which Li^+ binds stronger than Na^+ and K^+ and, as in olfactory cng channels, the ionic selectivity of the photoreceptor channel was not influenced by ligand concentration (Menini, 1990).

Inhibition by Cytosolic Acidification

Current inhibition by cytosolic acidification was not voltage dependent and was restricted to the cytosolic side of knob patches from frog and rat olfactory receptor cells. It seems, therefore, that one or more titratable groups reside on the cytosolic face of cng channels or on the membrane surface close to the channel opening, but apparently not within the pore structure. Protonation or screening of such a negatively charged group may change the surface potential in such a way that the local concentration of sodium in the vicinity of cng channels is diminished, resulting in a reduced conductance and smaller currents. Liebman, Mueller, and Pugh (1984) found a pH-induced suppression of the dark current in frog retinal rods with an apparent pK of 4.8, which they ascribed to the cytosolic side of the rod membrane. Menini and Nunn (1990) investigated pH effects on inside-out patches from rod outer segments where cytosolic acidification inhibited cGMP-activated current with an apparent pK of 5.4. In this preparation, the blockage by pH was also not voltage dependent.

It is difficult to assess whether this current inhibition by cytosolic acidification occurs under physiological conditions in olfactory receptor cells, for pH measurements in these cells have not been published yet. In photoreceptor cells, cytosolic pH does not change by more than 0.002 units during light excitation (Yoshikami and Hagins, 1985). It is, therefore, not to be expected that cytosolic pH has a direct regulatory function in cng channels of olfactory cilia, but the current inhibition observed demonstrates the presence of negatively charged groups near the channel opening with possible effects on ion permeation.

Inhibition by Organic Blockers

Amiloride blocked cng channels from frog and rat olfactory receptor cells from the cytosolic side of the membrane in most but not all patches. Previous results have shown that amiloride had no consistent effect on the cAMP-induced spike rate of most ORCs in the intact frog olfactory epithelium (Frings et al., 1991). However, odorant-induced rhythmic firing of action potentials (bursting) in isolated cells (Frings and Lindemann, 1988) was blocked by this drug. Apparently, amiloride can only gain access to ORCs when applied to the basolateral membrane of isolated cells, but not through the apical membrane of cells of intact tissue. If parts of the basolateral membrane are exposed to amiloride-containing solution, as in isolated cells, the drug may enter the cytosol and bind to the internal side of cng channels.

The pronounced sidedness of binding and the high K_i at physiological membrane voltages (>200 μM) make amiloride unsuited for extracellular application of intact ORCs, because the concentrations necessary to induce amiloride effects (0.1–1 mM; Persaud, DeSimone, Getchell, Heck, and Getchell, 1987) may also affect several other

transport systems and enzymes. In our experiments, the K_i at +60 mV was 32 μM in frog and 71 μM in rat cng channels. This is two orders of magnitude higher than the inhibition constant of epithelial Na channels (0.1–0.5 μM; Benos, 1982). It is similar to values found with Na/H exchangers and low threshold (T-type) Ca channels (3–80 μM; Benos, 1982; Zhuang, Cragoe, Shaikewitz, Glaser, and Cassel, 1984; Tang, Presser, and Morad, 1988), and considerably lower than K_i values of other Na transporters (Na/Ca exchanger: 1 mM [Bielefeld, Hadley, Vassilev, and Hume, 1986]; Na/K-ATPase: 3 mM [Soltoff and Mandel, 1983]; Na-glucose transporter: 2 mM [Kleyman and Cragoe, 1988]; voltage-sensitive Na channels: 0.6 mM [Kleyman and Cragoe, 1988]). Furthermore, the amiloride analogue 3′,4′-dichlorobenzamil is a more effective inhibitor than amiloride for both the cng channel (Nicol, Schnetkamp, Saimi, Cragoe, and Bownds, 1987; Kolesnikov et al., 1990) and the T-type Ca channel (Bielefeld et al., 1986), suggesting possible structural homologies between these two proteins.

A possible relation between cng channels and calcium channels is also supported by experiments with other Ca channel blockers. The phenylalkylamine D 600 (methoxyverapamil) and the benzothiazepine diltiazem, blockers of various types of Ca channels, inhibit cng channels in a voltage-dependent manner. There are, however, striking differences in how these blockers act on the two channel types. In Ca channels, concentrations for half-maximal blockage are 10–100 nM for phenylalkylamines and 50–1,000 nM for diltiazem (Reynolds and Snyder, 1988). K_i values in our experiments were up to two orders of magnitude higher, similar to concentrations necessary to block Ca-activated K channels (Gola and Ducreaux, 1985), delayed rectifier K channels (McDonald, Pelzer, and Trautwein, 1984), voltage-dependent Na channels (Triggle, 1981), and nicotinic acetylcholine receptors (Corcoran and Kirshner, 1983). The stereoselectivity of *l-cis-* over *d-cis*-diltiazem has been reported previously by Stern, Kaupp, and MacLeish (1986) and Schnetkamp (1990) in cng channels of photoreceptor cells and by Frings et al. (1991) in intact frog olfactory epithelium. This selectivity, together with the strong voltage sensitivity observed with all blockers, may indicate that inhibition by diltiazem is not "nonspecific" but that it involves interaction of the blocker with a binding site in the channel. Apparently, binding of diltiazem to the channel protein involves a distinct domain, different from the cGMP-binding domain, because after proteolytic treatment of cng channels purified from photoreceptors, sensitivity to *l-cis*-diltiazem was lost while activation by cGMP was sustained (Hurwitz and Holcombe, 1991). Interestingly, blockage of Ca channels by diltiazem has the inverse stereoselectivity, with *d-cis-* being eight times more potent than *l-cis*-diltiazem (Reynolds and Snyder, 1988).

In 2 out of 11 patches of rat knob membrane, cAMP-induced current was not blocked by amiloride. Thus, it seems possible that two different populations of cng channels exist in the sensory membrane of ORCs, showing different pharmacological properties. Nakamura and Gold (1987) found a subpopulation of cng channels with a dramatically reduced sensitivity to cAMP and cGMP in toad ORCs. Koch, Cook, and Kaupp (1987) also found evidence for two types of cng channels in bovine photoreceptors, only one of which was blocked by *l-cis*-diltiazem.

We thank Dr. G. Satzinger, Gödecke AG, Berlin, Germany, for the gift of *l-cis*-diltiazem and *d-cis*-diltiazem.

Support was received from the Deutsche Forschungsgemeinschaft through SFB 246, project Cl. J. W. Lynch was supported by a CSIRO postdoctoral award.

Original version received 27 November 1991 and accepted version received 15 April 1992.

REFERENCES

Almers, W., and E. W. McCleskey. 1984. The nonselective conductance in calcium channels of frog muscle: calcium selectivity in a single file pore. *Journal of Physiology.* 353:585–608.

Altenhofen, W., J. Ludwig, E. Eismann, W. Kraus, W. Bönigk, and U. B. Kaupp. 1991. Control of ligand-specificity in cyclic nucleotide-gated channels from rod photoreceptors and olfactory epithelium. *Proceedings of the National Academy of Sciences, USA.* 88:9868–9872.

Barry, P. H., and J. W. Lynch. 1991. Liquid junction potentials and small cell effects in patch-clamp analysis. *Journal of Membrane Biology.* 121:101–117.

Benos, D. J. 1982. Amiloride: a molecular probe of sodium transport in tissues and cells. *American Journal of Physiology.* 242:C131–C145.

Bielefeld, D. R., R. W. Hadley, P. M. Vassilev, and J. R. Hume. 1986. Membrane electrical properties of vesicular Na-Ca exchange inhibitors in single atrial myocytes. *Circulation Research.* 59:381–389.

Breer, H., I. Boekhoff, and E. Tareilus. 1990. Rapid kinetics of second messenger formation in olfactory transduction. *Nature.* 345:65–68.

Bruch, R. C., and J. H. Teeter. 1990. Cyclic AMP links amino acid chemoreceptors to ion channels in olfactory cilia. *Chemical Senses.* 15:419–430.

Colamartino, G., A. Menini, and V. Torre. 1991. Blockage and permeation of divalent cations through the cyclic GMP-activated channel from tiger salamander retinal rods. *Journal of Physiology.* 440:189–206.

Cook, N. J., C. Zeilinger, K.-W. Koch, and U. B. Kaupp. 1986. Solubilization and functional reconstitution of the cGMP-dependent cation channel from bovine rod outer segments. *Journal of Biological Chemistry.* 261:17033–17039.

Corcoran, J. J., and N. Kirshner. 1983. Inhibition of calcium uptake, sodium uptake, and catecholamine secretion by methoxyverapamil (D600) in primary cultures of adrenal medulla cells. *Journal of Neurochemistry.* 40:1106–1109.

Dhallan, R. S., K.-W. Yau, K. A. Schrader, and R. R. Reed. 1990. Primary structure and functional expression of a cyclic nucleotide-activated channel from olfactory neurons. *Nature.* 347:184–187.

Dryer, S. E., and D. Henderson. 1991. A cyclic GMP-activated channel in dissociated cells of the chick pineal gland. *Nature.* 353:756–758.

Eisenman, G., and R. Horn. 1983. Ionic selectivity revisited: the role of kinetic and equilibrium processes in ion permeation through channels. *Journal of Membrane Biology.* 76:197–225.

Firestein, S., and F. Werblin. 1989. Odor-induced membrane currents in vertebrate olfactory receptor neurons. *Science.* 244:79–82.

Firestein, S., F. Zufall, and G. M. Shepherd. 1991. Single odor-sensitive channels in olfactory receptor neurons are also gated by cyclic nucleotides. *The Journal of Neuroscience.* 11:3565–3572.

Frings, S., S. Benz, and B. Lindemann. 1991. Current recording from sensory cilia of olfactory receptor cells in situ. II. Role of mucosal Na^+, K^+, and Ca^{2+} ions. *Journal of General Physiology.* 97:725–747.

Frings, S., and B. Lindemann. 1988. Odorant response of isolated olfactory receptor cells is blocked by amiloride. *Journal of Membrane Biology.* 105:233–243.

Frings, S., and B. Lindemann. 1991*a*. Current recording from sensory cilia of olfactory receptor cells in situ. I. The neuronal response to cyclic nucleotides. *Journal of General Physiology.* 97:1–16.

Frings, S., and B. Lindemann. 1991*b*. Properties of cyclic nucleotide-gated channels mediating olfactory transduction: sidedness of voltage-dependent blockage by Ca^{2+} ions, amiloride, D600, and diltiazem. *Journal of General Physiology*. 98:17*a*. (Abstr.)

Furman, R. E., and J. C. Tanaka. 1990. Monovalent selectivity of the cyclic guanosine monophosphate-activated ion channel. *Journal of General Physiology*. 96:57–82.

Gola, M., and C. Ducreaux. 1985. D600 as a direct blocker of Ca-dependent K currents in *Helix* neurons. *European Journal of Pharmacology*. 117:311–322.

Goulding, E., J. Ngai, R. Kramer, S. Colicos, R. Axel, S. Siegelbaum, and A. Chess. 1992. Molecular cloning and single-channel properties of the cyclic nucleotide-gated channel from catfish olfactory neurons. *Neuron*. 8:45–58.

Hamill, O. P., A. Marty, E. Neher, B. Sakmann, and F. J. Sigworth. 1981. Improved patch-clamp techniques for high-resolution current recording from cells and cell-free membrane patches. *Pflügers Archiv*. 391:85–100.

Hanke, W., N. J. Cook, and U. B. Kaupp. 1988. cGMP-dependent channel protein from photoreceptor membrane: single channel activity of the purified and reconstituted protein. *Proceedings of the National Academy of Sciences, USA*. 85:94–98.

Haynes, L. W., A. R. Kay, and K.-W. Yau. 1986. Single cyclic GMP-activated channel activity in excised patches of rod outer segment membrane. *Nature*. 321:66–70.

Haynes, L. W., and K.-W. Yau. 1990. Single-channel measurement from the cyclic GMP-activated conductance of catfish retinal cones. *Journal of Physiology*. 429:451–481.

Hess, P., and R. W. Tsien. 1984. Mechanism of ion permeation through calcium channels. *Nature*. 309:453–456.

Hodgkin, A. L., P. A. McLaughton, and B. J. Nunn. 1985. The ionic selectivity and calcium dependence of the light-sensitive pathway in toad rods. *Journal of Physiology*. 358:447–468.

Hurwitz, R., and V. Holcombe. 1991. Affinity purification of the photoreceptor cGMP-gated cation channel. *The Journal of Biological Chemistry*. 266:7975–7977.

Ildefonse, M., and N. Bennett. 1991. Single-channel study of the cGMP-dependent conductance of retinal rods from incorporation of native vesicles into planar lipid bilayers. *Journal of Membrane Biology*. 123:133–147.

Karpen, J. W., A. L. Zimmerman, L. Stryer, and D. A. Baylor. 1988. Gating kinetics of the cGMP-activated channel of retinal rods: flash photolysis and voltage-jump studies. *Proceedings of the National Academy of Sciences, USA*. 85:1287–1291.

Kaupp, U. B. 1991. The cyclic nucleotide-gated channels of vertebrate photoreceptors and olfactory epithelium. *Trends in Neurosciences*. 14:150–157.

Kaupp, U. B., T. Niidome, T. Tanabe, S. Terada, W. Bönigk, W. Stühmer, N. J. Cook, K. Kangawa, H. Matsuo, T. Hirose, T. Miyata, and S. Numa. 1989. Primary structure and functional expression from complementary DNA of the rod photoreceptor cyclic GMP-gated channel. *Nature*. 342:762–766.

Kleyman, T. R., and E. J. Cragoe, Jr. 1988. Amiloride and its analogs as tools in the study of ion transport. *Journal of Membrane Biology*. 105:1–21.

Koch, K.-W., N. J. Cook, and U. B. Kaupp. 1987. The cGMP-dependent channel of vertebrate rod photoreceptors exists in two forms of different cGMP sensitivity and pharmacological behavior. *The Journal of Biological Chemistry*. 262:14415–14421.

Kolesnikov, S. S., T. I. Rebrik, A. B. Zhaiazarov, G. A. Tavartkiladze, and G. R. Kalamkarov. 1991. A cyclic-AMP-gated conductance in cochlear hair cells. *FEBS Letters*. 290:167–170.

Kolesnikov, S. S., A. B. Zhainazarov, and A. V. Kosolapov. 1990. Cyclic nucleotide-activated channels in the frog olfactory receptor plasma membrane. *FEBS Letters*. 266:96–98.

Kurahashi, T. 1990. The response induced by intracellular cyclic AMP in isolated olfactory receptor cells of the newt. *Journal of Physiology.* 430:355–371.

Kurahashi, T., and A. Kaneko. 1991. High density cAMP-gated channels at the ciliary membrane in the olfactory receptor cell. *NeuroReport.* 2:5–8.

Liebman, P. A., P. Mueller, and E. N. Pugh, Jr. 1984. Protons suppress the dark current of frog retinal rods. *Journal of Physiology.* 347:85–110.

Lowe, G., and G. H. Gold. 1991. The spatial distributions of odorant sensitivity and odorant-induced currents in salamander olfactory receptor cells. *Journal of Physiology.* 442:147–168.

Lowe, G., T. Nakamura, and G. H. Gold. 1989. Adenylate cyclase mediates olfactory transduction for a wide variety of odorants. *Proceedings of the National Academy of Sciences, USA.* 86:5641–5645.

Ludwig, J., T. Margalit, E. Eismann, D. Lancet, and U. B. Kaupp. 1990. Primary structure of cAMP-gated channel from bovine olfactory epithelium. *FEBS Letters.* 270:24–29.

Lühring, H., W. Hanke, R. Simmoteit, and U. B. Kaupp. 1990. Cation selectivity of the cGMP-gated channel of mammalian rod photoreceptors. *In* Sensory Transduction. A. Borsellino, L. Cervetto, and V. Torre, editors. Plenum Publishing Corp., New York. 169–173.

Lynch, J. W., and P. H. Barry. 1991. Properties of transient K^+ currents and underlying single K^+ channels in rat olfactory receptor neurons. *Journal of General Physiology.* 97:1043–1072.

Matthews, G. 1987. Single-channel recordings demonstrate that cGMP opens the light-sensitive ion channel of the rod photoreceptor. *Proceedings of the National Academy of Sciences, USA.* 84:299–302.

McDonald, T. F., D. Pelzer, and W. Trautwein. 1984. Cat ventricular muscle treated with D600: Effect on calcium and potassium currents. *Journal of Physiology.* 352:203–216.

Menco, B. P. M. 1980. Qualitative and quantitative freeze-fracture studies on olfactory and nasal respiratory epithelial surfaces of frog, ox, rat, and dog. *Cell Tissue Research.* 211:5–29.

Menini, A. 1990. Currents carried by monovalent cations through cyclic GMP-activated channels in excised patches from salamander rods. *Journal of Physiology.* 424:167–185.

Menini, A., and B. J. Nunn. 1990. The effect of pH on the cyclic GMP-activated conductance in retinal rods. *In* Sensory Transduction. A. Borsellino, L. Cervetto, and V. Torre, editors. Plenum Publishing Corp., New York. 175–181.

Miller, J. P., A. H. Beck, L. N. Simon, and R. B. Meyer, Jr. 1975. Induction of hepatic tyrosine aminotransferase *in vivo* by derivatives of cyclic adenosine 3′:5′-monophosphate. *The Journal of Biological Chemistry.* 250:426–431.

Molday, R. S., L. L. Molday, A. Dosé, I. Clark-Lewis, M. Illing, N. J. Cook, E. Eismann, and U. B. Kaupp. 1991. The cGMP-gated channel of the rod photoreceptor cell. Characterization and orientation of the amino terminus. *The Journal of Biological Chemistry.* 266:21917–21922.

Nakamura, T., and G. H. Gold. 1987. A cyclic nucleotide-gated conductance in olfactory receptor cilia. *Nature.* 325:442–444.

Nicol, G. D., P. P. M. Schnetkamp, Y. Saimi, E. J. Cragoe, Jr., and M. D. Bownds. 1987. A derivative of amiloride blocks both the light-regulated and cyclic GMP-regulated conductances in rod photoreceptors. *Journal of General Physiology.* 90:651–669.

Pace, U., E. Hanski, Y. Salomon, and D. Lancet. 1985. Odorant-sensitive adenylate cyclase may mediate olfactory reception. *Nature.* 316:255–258.

Persaud, K. C., J. A. DeSimone, M. L. Getchell, G. L. Heck, and T. V. Getchell. 1987. Ion transport across the frog olfactory mucosa: the basal and odorant-stimulated states. *Biochimica et Biophysica Acta.* 902:65–79.

Quandt, F. N., G. D. Nicol, and P. P. M. Schnetkamp. 1991. Voltage-dependent gating and block of the cyclic GMP-dependent current in bovine rod outer segments. *Neuroscience.* 42:629–638.

Reese, T. S. 1965. Olfactory cilia in the frog. *Journal of Cell Biology.* 25:209–230.

Reynolds, I. J., and S. H. Snyder. 1988. Calcium antagonist receptors. *In* Ion Channels. T. Narahashi, editor. Plenum Publishing Corp., New York. 213–249.

Schnetkamp, P. P. M. 1990. Cation selectivity of and cation binding to the cGMP-dependent channel in bovine rod outer segment membranes. *Journal of General Physiology.* 96:517–534.

Sklar, P. B., R. R. H. Anholt, and S. H. Snyder. 1986. The odorant-sensitive adenylate cyclase of olfactory receptor cells. *The Journal of Biological Chemistry.* 261:15538–15543.

Soltoff, S. P., and L. J. Mandel. 1983. Amiloride directly inhibits the Na,K-ATPase activity of rabbit kidney proximal tubules. *Science.* 220:957–958.

Stern, J. H., U. B. Kaupp, and P. R. MacLeish. 1986. Control of light-regulated current in rod photoreceptors by cyclic GMP, calcium, and *l-cis*-diltiazem. *Proceedings of the National Academy of Sciences, USA.* 83:1163–1167.

Suzuki, N. 1988. Cation selectivity of cyclic nucleotide-gated conductance in isolated olfactory receptor cells. *Zoological Sciences.* 5:1194. (Abstr.)

Suzuki, N. 1989. Voltage- and cyclic nucleotide-gated currents in isolated olfactory receptor cells. *In* Chemical Senses. Vol. 1. J. G. Brand, J. H. Teeter, R. H. Cagan, and M. R. Kare, editors. Marcel Dekker, Inc., New York. 469–493.

Tang, C.-M., F. Presser, and M. Morad. 1988. Amiloride selectively blocks the low threshold (T) calcium channel. *Science.* 240:213–215.

Triggle, D. J. 1981. Calcium antagonists: basic chemical and pharmacological aspects. *In* New Perspectives on Calcium Antagonists. G. B. Weiss, editor. American Physiological Society, Bethesda, MD. 1–18.

Trotier, D., and P. MacLeod. 1986. cAMP and cGMP open channels and depolarize olfactory receptor cells. *Chemical Senses.* 11:674. (Abstr.)

Yau, K. W., and D. A. Baylor. 1989. Cyclic GMP-activated conductance of retinal photoreceptor cells. *Annual Review of Neuroscience.* 12:289–327.

Yoshikami, S., and W. A. Hagins. 1985. Cytoplasmic pH in rod outer segments and high energy phosphate metabolism during phototransduction. *Biophysical Journal.* 47:101*a*. (Abstr.)

Zhuang, Y.-X., E. J. Cragoe, Jr., T. Shaikewitz, L. Glaser, and D. Cassel. 1984. Characterization of potent Na^+/H^+ exchange inhibitors from the amiloride series in A431 cells. *Biochemistry.* 23:4481–4488.

Zimmerman, A. L., and D. A. Baylor. 1986. Cyclic GMP-sensitive conductance of retinal rods consists of aqueous pores. *Nature.* 321:70–72.

Zimmerman, A. L., G. Yamanaka, F. Eckstein, and D. A. Baylor. 1985. Interaction of hydrolysis-resistant analogs of cyclic GMP with the phosphodiesterase and light-sensitive channel of retinal rod outer segment. *Proceedings of the National Academy of Sciences, USA.* 82:8813–8817.

Zufall, F., S. Firestein, and G. M. Shepherd. 1991. Analysis of single nucleotide-gated channels in olfactory receptor cells. *The Journal of Neuroscience.* 11:3573–3580.

Zufall, F., G. M. Shepherd, and S. Firestein. 1991. Inhibition of the olfactory cyclic nucleotide gated ion channel by intracellular calcium. *Proceedings of the Royal Society of London, B.* 246:225–230.